Influence of Nanoxides on Diffusivity and Solubility of Hydrogen in Pd-based alloys

Tabatta Regina de Brito Martins[a]*, Viviane Monteiro Azambuja[b], Dilson Silva dos Santos[a,c], Sérgio

Souto Maior Tavares[d]

[a]Programa de Engenharia da Nanotecnologia, Universidade Federal do Rio de Janeiro - UFRJ, Rio de Janeiro, RJ, Brazil
[b]Instituto Federal de Educação Ciência e Tecnologia do Espírito Santo - IFES, Vitória, ES, Brazil
[c]Departmento de Engenharia Metalúrgica e de Materiais, Universidade Federal do Rio de Janeiro - UFRJ, Rio de Janeiro, RJ, Brazil
[d]Departamento de Engenharia Mecânica, Universidade Federal Fluminense - UFF, Niterói, Rio de Janeiro, Brazil

The hydrogen interaction in palladium alloys with addition of Ce, Zr and Y was studied. These alloys are produced by arc-melting and then cold rolled into thin foils. Heat treatment at 800ºC for 24h in air atmosphere is applied to induce internal oxidation. Hydrogen permeation tests and TDS (Thermal Desorption Spectroscopy) are carried out to evaluate hydrogen interaction with three different microstructures which can be characterized by dislocations, substitutional atoms and nanoxides. For alloys argon annealed, Ce is the element that delays the most hydrogen diffusion, followed by Zr and Y. However alloys with yttrium nanoxides exhibit the highest solubility and the smallest diffusivity due to their small size, spherical shape and dispersion throughout the matrix. Analyzing TDS curves, it is shown that nanoxides are irreversible traps that improve hydrogen stored on palladium alloys. Dislocations and impurity atom on solid solution have little binding energy that detraps hydrogen at smaller temperatures.

Keywords: *nanoxides, internally oxidation, palladium, diffusivity of hydrogen, solubility of hydrogen.*

1. Introduction

Pd alloys are a noble and costly metal; however, they have special characteristics with regard to hydrogen, such as: excellent kinetics of adsorption and absorption of hydrogen, durability as a function of hydrogen loading and unloading, as well as good mechanical resistance when there is formation of the hydride phase. Pd-H system has many engineering applications, such as fuel cells, filters and hydrogen separators; can also be used as hydrogen storage tanks and catalysts. Thus Pd alloys are so studied by science and engineering[1,2]. In addition, the palladium alloys are widely used to understand the interaction of hydrogen with the crystalline defects, precisely because of all these presented properties.

Microstructure plays such an important role on hydrogen diffusion and solubility. Dislocations, vacancies, grain boundary, substitutional and interstitial atoms, and interfaces induce distortions and high energy fields on crystalline structure. These defects are preferable sites to hydrogen trapping. The nature of this interaction between hydrogen and a given microstructure defines whether a trap is reversible or irreversible[3]. Despite the hydrogen diffusion through the lattice is independent of the trap sites, this amount delays

hydrogen permeation, because the permeation only starts after all trappings are filled. Therefore the hydrogen permeation is delayed because hydrogen trap sites on matrix. Cao and coworkers[10] investigated the relationship between amount of cold work, dislocation density and hydrogen diffusion, they concluded that when increasing the amount of deformation in palladium, the dislocation density also increased, and hydrogen permeation in palladium is delayed even more.

PdX alloys where X is an element which interacts strongly with oxygen (such as Y, Zr, Ce, Al, Cu) can be heat treated to obtain nanoxides on Pd lattice. This occurs when these alloys are exposed to an oxidizing atmosphere at high temperature for extended treatment times, sufficient to permit the oxygen diffusion through the metallic matrix. Such oxides promote an increase in hydrogen solubility as well as improve the mechanical properties of these alloys[4-6].

In this sense, this paper presents how different microstructures promote drastic changes in the diffusivity and solubility of hydrogen. PdX alloys were arc-melted, cold rolled and heat treated to make three different samples: argon annealed (substitutional atom on Pd lattice), cold worked (combine effect of substitutional atom on Pd lattice and dislocations) and internally oxidized (nanoxides interfaces). X-ray diffraction, SEM (Scanning Electron Microscopy) and

TEM (Transmission Electron Microscopy) were performed to characterize the samples. Hydrogen permeation tests and TDS (Thermal Desorption Spectroscopy) were carried out to investigate hydrogen interaction with these microstructures. The microstructure with the lowest diffusion coefficient is the internally oxidized. Among the studied PdX alloys, the one containing yttrium oxide is the alloy with the lowest diffusion coefficient, followed by the one with zirconium oxide and the last one containing cerium oxide. This delay in the hydrogen permeation is related to the morphology of the oxides, their size and distribution.

2. Materials and Experimental Methods

With the purpose of investigating the interaction between hydrogen and cerium, zirconium or yttrium nanoxides, some $Pd_{0.97}X_{0.03}$ alloys were prepared, from the commercial pure elements by arc-melting. Subsequently, all buttons of alloys, with about 15mm in diameter, were cold rolled in six passes into a thin foil (200 µm) and three different samples of each one were separated, where the first was named $Pd_{0.97}X_{0.03}$ CW (cold worked) and the others were heat treated at 800ºC per 24h under argon and air atmospheres, producing respectively, $Pd_{0.97}X_{0.03}$ AA (argon annealed) and $Pd_{0.97}X_{0.03}$ IO (internally oxidized). As Cao and coworkers[10] demonstrated, the quantity of cold work intervenes on hydrogen diffusion, so that the same amount of cold work was imposed on all alloys studied. Figure 1 shows the sample preparation flowchart. The heat treatment under argon produced alloys without dislocations begotten by cold work, whereas an internal oxidation was performanced due to reactive atmosphere. Therefore, the sample $Pd_{0.97}X_{0.03}$ AA allowed studying the effect of a substitutional atom on hydrogen trapping, while $Pd_{0.97}X_{0.03}$ CW let a combined action of a substitutional atom and dislocations. The last sample highlighted the hydrogen interaction only with nanoxides.

Samples of 15 x 15 mm dimension were submitted to electrochemical hydrogen permeation tests, at room temperature, using a 0.1 M NaOH solution as electrolyte as described elsewhere[7]. These tests were undertaken using an electrochemical cell comprising two compartments separated by the sample. In one of them, a constant cathodic current was applied to generate hydrogen at the surface of the metal

foil. In the other compartment, a weak anodic potential was applied to oxidize the hydrogen that permeates through the sample. For each sample, two cycles of sorption-desorption were applied to promote the saturation of the trap sites. The cathodic current used was 1 mA.

Before and after permeation tests, the resulting samples were characterized by a X-ray diffraction with the use of Bruker D8 discovery diffractometer which operated with Cu Kα radiation.

The surface of the alloys was observed by SEM and microanalyses were performed by EDS (Energy Dispersive X-ray Spectrometer). The grain boundaries were visible due to internally oxidation, even without etching. Furthermore, the nanoxides morphology were analyzed by TEM operating at 200 kV and equipped with an energy dispersive X-ray spectrometry for microanalysis (EDS). The disks with 3 mm in diameter were then carefully polished to a thickness of about 80 µm. Then specimens were prepared by dual jet electropolishing using a Struers Tenupol-5 electropolisher with an electrolyte composed of 91 vol.% acetic acid and 9 vol.% perchloric acid at 15ºC and a voltage of 20.5 V against a Pt counter electrode.

The nature of hydrogen traps in PdY alloys was investigated by thermal desorption spectroscopy (TDS) with heating rate of 10ºC/min from the room temperature until 600ºC. Before the tests, electrochemical hydrogen charging was performed from 0.1 M NaOH solution with 0.3 A/cm² during 24h.

3. Results and Discussion

Figure 2 presents X-ray diffraction patterns for $Pd_{0.97}Y_{0.03}$ CW and for $Pd_{0.97}Y_{0.03}$ IO. It was observed that the CW sample presented only peaks due to a palladium face-centered cubic (FCC) structure with yttrium in solid solution. However, for the IO sample, other diffraction peaks were observed. These new peaks were indexed as Y_2O_3 and PdO, this last one was really small. Since yttrium has more affinity with oxygen than palladium, there are more pronounced Y_2O_3 peaks. The other alloys have X-ray diffraction patterns very similar to these, the only difference is the oxides formed: CeO_2 and ZrO_2 for $Pd_{0.97}Ce_{0.03}$ and $Pd_{0.97}Zr_{0.03}$, respectively.

Figure 3 refers to the SEM analysis of the $Pd_{0.97}Y_{0.03}$ IO alloy and some points were chosen to carry out microanalyses
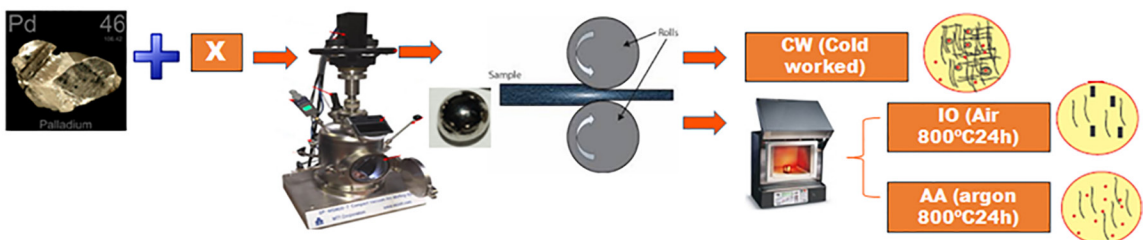

Figure 1. Sample preparation flowchart, where X is Ce, Zr or Y. The heat treatment in air produced internal oxidation (IO condition) and the argon annealing lead to a microstructure with X atoms in substitutional solution solid.
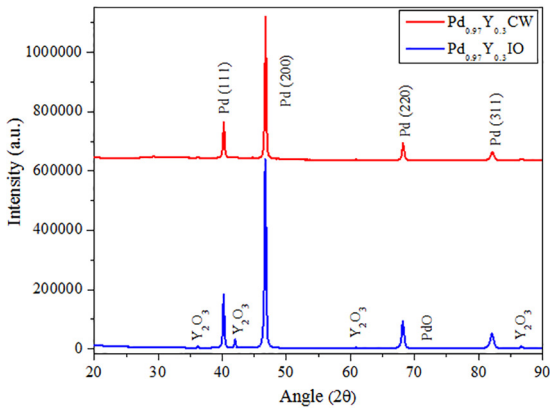
Figure 2. X-ray diffraction patterns for the $Pd_{0.97}Y_{0.03}$ alloy: cold worked and oxidized at 800ºC per 24h.

by EDS. The same procedure was done for all alloys and made resembling pictures. It can be noticed that point 1 (in grain boundary) presents an oxygen peak and more pronounced yttrium peak when compared with point 2 (on matrix). This difference between point 1 and 2 shows that yttrium oxide forms preferably in grain boundary and a little amount of it remains in solid solution in Pd lattice. Therefore, the internal oxidation was not complete and oxides still stay small enough to be a good hydrogen trap. As it is known when the oxides increase greatly in size they cease to be an efficient trap for hydrogen[8].
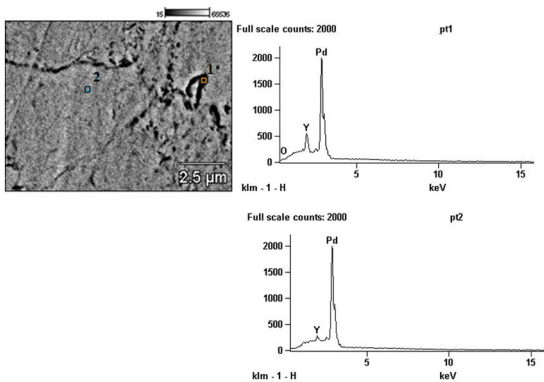
Figure 3. SEM image and EDS for $Pd_{0.97}Y_{0.03}$ oxidized at 800ºC during 24h.

Figure 4 (a-b) shows a TEM and SEM photomicrograph of $Pd_{0.97}Ce_{0.03}$ IO alloy where the fine acicular ceria precipitates (arrows) of 20-40 nm in diameter and 1-2 µm in length can be seen[6]. These precipitates exhibited preferential growth directions. Through the diffraction picture it was possible to index the precipitates being CeO_2 with crystalline parameter of $a_0 = 5.41$ Å, which have a coherence relation with the palladium matrix[6].

As it can be seen in Figures 5-6, zirconium oxide precipitates in grain boundaries with nanometric size of approximately 15 nm and almost a square shape (see arrows).
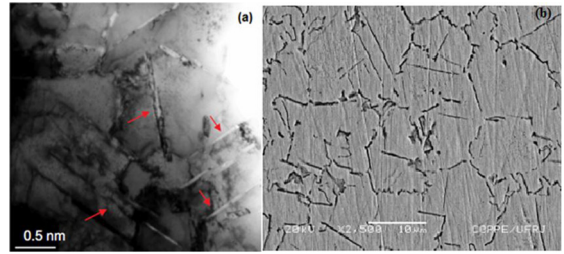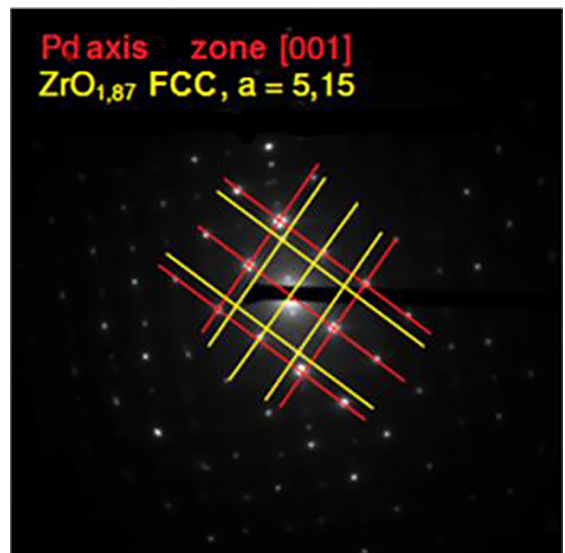

Figure 4. Transmission electron micrograph for $Pd_{0.97}Ce_{0.03}$ IO[6] (a) and SEM (b).

The zirconium oxide could be indexed as $ZrO_{1.87}$, with face centered cubic (FCC) structure and lattice parameter $a_0 = 5.15$ Å. It can also be verified that zirconium oxide, as the cerium oxide, is coherent with the palladium matrix. The yttrium oxides were also investigated (Figure 7) and it was possible observed that their shape is spherical with nanometric size of approximately 10 nm similar to zirconium oxides, but smaller and spherical.
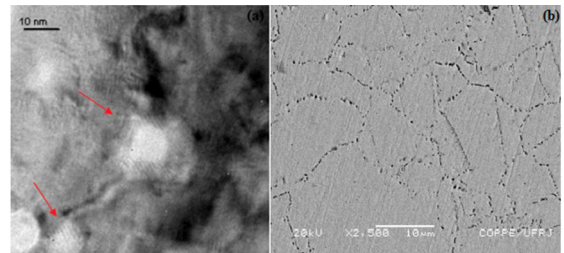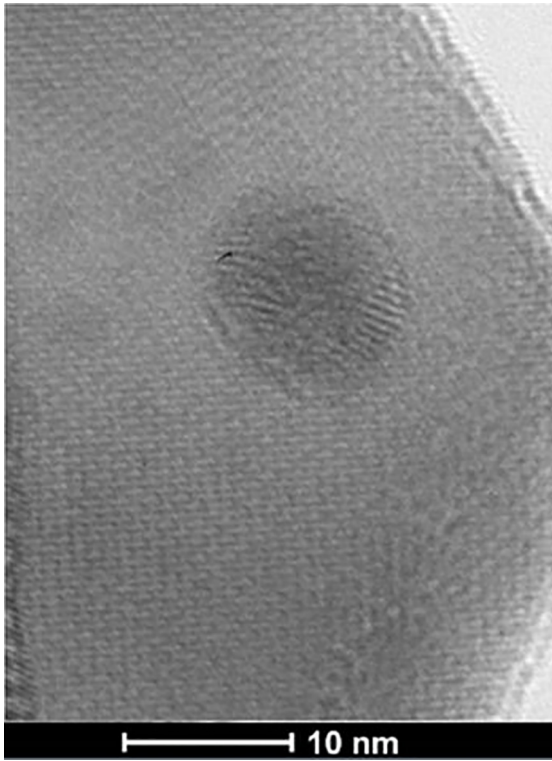

Figure 5. Transmission electron micrograph for $Pd_{0.97}Zr_{0.03}$ IO (a) and SEM (b).

Figure 6. Transmission electron micrograph of selected region electron diffraction pattern for $Pd_{0.97}Zr_{0.03}$ IO.

Figure 8 (a-c) shows the hydrogen permeation curves for the $Pd_{0.97}X_{0.03}$. The curves were normalized by the value of maximum flux of each curve. In Table 1 the hydrogen

Figure 7. Transmission electron micrograph for $Pd_{0.97}Y_{0.03}$ IO, showing a spherical yttrium nanoxide.

Table 1. Hydrogen permeation parameters of pure Pd and Pd alloys at 313 K for cathodic charging current equal to 1 mA.

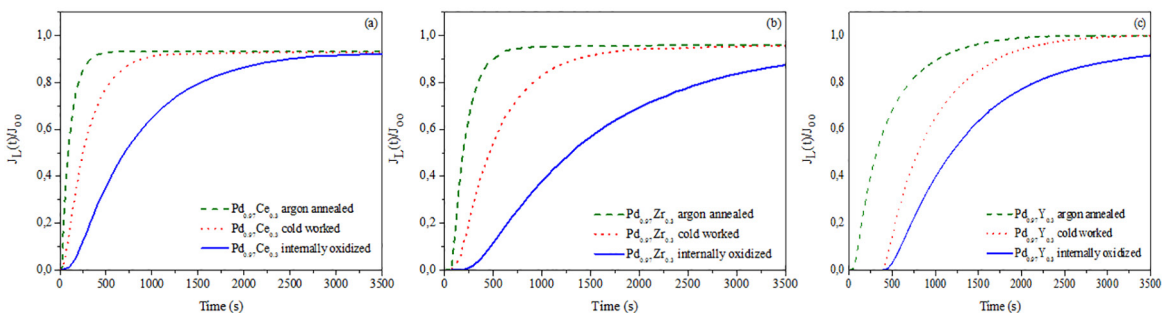| Alloys	D_{app} (m^2.s^{-1})	S_{app} (mol H m^{-3})	J_{∞} (mol H m^{-2}s^{-1})
Pd CW	2.6×10^{-11}	1730	1.86×10^{-4}
$Pd_{0.97}Ce_{0.03}$AA	3.3×10^{-11}	758	1.96×10^{-4}
$Pd_{0.97}Ce_{0.03}$CW	1.9×10^{-11}	1147	2.18×10^{-4}
$Pd_{0.97}Ce_{0.03}$IO	6.0×10^{-12}	2863	1.95×10^{-4}
$Pd_{0.97}Zr_{0.03}$AA	4.3×10^{-11}	761	1.43×10^{-4}
$Pd_{0.97}Zr_{0.03}$CW	1.1×10^{-11}	2081	2.19×10^{-4}
$Pd_{0.97}Zr_{0.03}$IO	3.0×10^{-12}	5228	2.19×10^{-4}
$Pd_{0.97}Y_{0.03}$AA	5.2×10^{-11}	501	2.12×10^{-4}
$Pd_{0.97}Y_{0.03}$CW	6.6×10^{-12}	5280	1.76×10^{-4}
$Pd_{0.97}Y_{0.03}$IO	2.5×10^{-12}	7783	1.51×10^{-4}

factors such as valence and stressing must also be considered because different metal valences and an external stress field can improve the hydrogen solubility[1,2,9].

It was also shown, from Table 1, that cold work decreases hydrogen diffusion coefficient. This could be due to the multiplication of dislocations and generation of vacancies during deformation which trap the hydrogen in a reversible or an irreversible way depending on defect binding energy[10]. Besides that, when element X in solid solution is combined with cold work, the hydrogen diffusion coefficient is further lowered, in comparison to pure Pd CW ($D_{app} = 2.6 \times 10^{-11}$ m^2.s^{-1}). For X=Ce (alloy $Pd_{0.97}Ce_{0.03}$ CW) the decrease of diffusivity was 37%, while for X=Y (alloy $Pd_{0.97}Y_{0.03}$ CW) a decrease of 300% in the D_{app} was measured.

In spite of the difference between atomic rays predominates on hydrogen diffusion coefficient for annealed alloys, the same does not happen for CW and IO ones. Yttrium is the element that most delayed the hydrogen permeation for CW and IO conditions; this reduction in the D_{app} reaches 96% and 99%, respectively. For cold worked samples, it happens because bigger atoms are better barriers to dislocations motions, preventing, this way, multiplication of dislocation. Therefore, $Pd_{0.97}Ce_{0.03}$ and $Pd_{0.97}Zr_{0.03}$ alloys must have lower dislocation densities than $Pd_{0.97}Y_{0.03}$.

The diffusivity of hydrogen is inversely proportional to difference atomic rays between Pd and X element, for

permeation parameters of the alloys are compared with those of pure Pd cold worked (CW).

Analyzing Figure 8 and Table 1 data, it can be observed that the addition of Ce, Zr, or Y in Pd lattice induces an increase in the hydrogen permeation time, which represents a decrease on diffusivity of hydrogen. This reduction is less pronounced for the PdX AA than PdX CW or PdX IO. Pure Pd has $D_{app} = 5.5 \times 10^{-11}$ m^2.s^{-1} and when Ce, Zr or Y are added in Pd lattice, its diffusivity is reduced. For the AA condition, this behavior can be explained by lattice distortion caused by the X element in solid solution. As Y possesses an atomic radius closer to Pd, the distortion due to physical nature is smaller than in the case of Zr and Ce where the atomic radius is greater than Pd and Y. This effect was observed for other Pd alloys. Furthermore, other

Figure 8. Hydrogen permeation curves with 1.0 mA: $Pd_{0.97}Ce_{0.03}$ (a); $Pd_{0.97}Zr_{0.03}$ (b) and $Pd_{0.97}Y_{0.03}$ (c).

oxidized condition. This behavior can be explained on the basis of the shape, size and location of the oxides precipitated in each alloy[8,11]. Ytrium and zirconium oxides have almost similar size, but different shape, spherical for Y oxide, and near square for Zr oxide. In addition, Zr oxides precipitate preferably at grain boundaries, while Y ones are more dispersed in the matrix. Despite of these differences, the Y and Zr oxides seem to produce similar effects on the H diffusivity, because the D_{app} of $Pd_{0.97}Y_{0.03}$ IO (2.5×10^{-12} $m^2.s^{-1}$) and $Pd_{0.97}Zr_{0.03}$ IO (3.0×10^{-12} $m^2.s^{-1}$) alloys are very close. On the other hand, the Ce oxide precipitated in $Pd_{0.97}Ce_{0.03}$ IO alloy, with the acicular shape shown in Figs. 4(a-b), has a less effective trapping effect ($D_{app} = 6.0 \times 10^{-12}$ $m^2.s^{-1}$).

Moreover, the solubility has an inverse behavior in comparison with the diffusivity for all cases discussed (Table 1). It is observed that IO is the condition that maximizes the amount of stored hydrogen, followed by CW one. This raise occurs because the oxide matrix interface has higher binding energy than dislocations, so that it is probably an irreversible trap that enabling, this way, higher solubility.

Hydrogen release and detrapping from the metals, during heating processes were studied by means of thermal desorption spectroscopy (TDS). Typical TDS curves (for the heating rate 10ºC/min) for all three conditions of studied $Pd_{0.97}Y_{0.03}$ alloys can be compared with Pd CW in Figure 9. Differences in the microstructure of the studied condition noticeably influence the shape and height of the observed TDS peaks, as well as the temperature of the peaks.
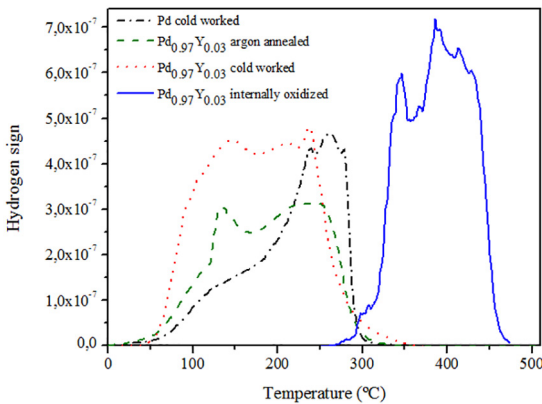
Figure 9. TDS spectra for hydrogen release from $Pd_{0.97}Y_{0.03}$ alloys.

The TDS spectrum, measured for Pd CW revealed three well-defined peaks at 238, 261 and 278ºC. Kirchheim[12] and co-workers reported that hydrogen desorption occurs from: octahedral sites, reversible and irreversible trappings, in that order, as the temperature increasing. So that, this peaks in palladium could be attributed to diffusible hydrogen, dislocations and hydrides. As $Pd_{0.97}Y_{0.03}$ CW samples exhibit similar TDS spectrum to Pd CW, their peaks can be characterized in the same way.

Nevertheless for AA condition, there are only two peaks, located at 137 and 246ºC. The missing peak corresponds to dislocations, because heat treatment annihilates the most of them. Analysis of TDS spectra for $Pd_{0.97}Y_{0.03}$ IO, reveals at least four well-defined peaks at 303, 347, 386 and 412ºC. This more complex format is probably due to yttrium oxides precipitated in grain boundaries and dispersed in the matrix.

The displacement of the temperature peaks between IO and the other conditions ratifies the irreversible nature of the oxides in hydrogen trapping. TDS graphic presents similar shapes for $Pd_{0.97}Y_{0.03}$ AA, CW and Pd CW, because of reversible hydrogen trapping on dislocations and impurity atoms. CW samples have curves with higher height peaks than argon annealed condition. This occur owing combined effect of dislocations and substitutional atoms or hydride formation.

4. Summary and Conclusions

This study aimed to investigate the influence of the different microstructures, such as: substitutional atoms, dislocations and nanoxides with different morphologies. Thus, the results found can be summarized as follows:

- Air heat treatment at 800ºC for 24h promotes internally oxidation of Ce, Zr and Y leading to nanoxides precipitates. Cerium and zirconium oxides have similar stoichiometry but the morphology of the first one is fine acicular. Both are coherent with the palladium matrix. While the oxides of Y and Zr have almost the same size and resembling shapes.

- Cerium is the element that lowers the most the diffusivity of hydrogen whereas yttrium lead to the highest one for argon annealed condition. Nevertheless all values are smaller when compared with pure Pd.

- The oxide precipitation induces a significant increase in hydrogen storage. Alloys with yttrium nanoxides present the highest solubility, followed by ZrO_2 and CeO_2. This behavior can be explained based on the shape, size and distribution of the oxides. Yttrium oxide has the lowest diffusion coefficient, due to its morphology (the smallest spherical nanoxide).

- TDS curves for cold worked (CW) and argon annealed (AA) have similar shape and present near temperature range. However internally oxidized (IO) spectra has a more complex format with higher temperatures.

- Nanoxides are irreversible traps that improve hydrogen stored on palladium alloys. Dislocations and impurity atoms on solid solution have little binding energy that detraps hydrogen at smaller temperatures.

Acknowledgements

6. References

1. Gesari SB, Prosanto ME, Juan A. Simulation of hydrogen trapping at defects in Pd. *International Journal of Hydrogen Energy*. 2009;34(8):3511-3518.

2. Iwaoka H, Arita M, Horita Z. Hydrogen diffusion in ultrafine-grained palladium: Roles of dislocations and grain boundaries. *Acta Materialia*. 2016;107:168-177.

3. Michler T, Balogh MP. Hydrogen environment embrittlement of an ODS RAF steel - Role of irreversible hydrogen trap sites. *International Journal of Hydrogen Energy*. 2010;35(18):9746-9754.

4. Jose D, Jagirdar BR. Nature of hydrogen atom trapped inside palladium lattice. *International Journal of Hydrogen Energy*. 2010;35(13):6804-6811.

5. Zhang W, Luo S, Wang D, Flanagan TB, Balasubramaniam R. Hydrogen segregation to internal interfaces of Pd-yttria composite prepared by internal oxidation of Pd-Y alloys. *Journal of Alloys and Compounds*. 2002;330-332:607-611.

6. Azambuja VM, Dos Santos DS, Pontonnier L, Morales M, Fruchart D. Study of an internally-oxidized $Pd_{0.97}Ce_{0.03}$ alloy. *Scripta Materialia*. 2006;54(10):1779-1783.

7. Dos Santos DS, de Miranda PEV. The use of electrochemical hydrogen permeation techniques to detect hydride phase separation in amorphous metallic alloys. *Journal of Non-Crystalline Solids*. 1998;232-234:133-139.

8. Balasubramaniam R, Noh H, Flanagan TB, Sakamoto Y. Hydrogen solubility in Pd/Al_2O_3 composites prepared by internal oxidation of Pd-Al alloys. *Acta Materialia*. 1997;45(4):1725-1733.

9. Kirchheim R, McLellan RB. Diffusivity of hydrogen in dilute alloys of copper and niobium in palladium. *Acta Metallurgica*. 1982;28(11):1549-1554.

10. Cao Y, Li HL, Szpunar JA, Shmayda W. Modeling of hydrogen trapping in the deformed Pd and $Pd_{77}Ag_{23}$ alloy. *Materials Science and Engineering: A*. 2004;379(1-2):173-180.

11. Gouthama G, Balasubramaniam R, Wang D, Flanagan TB. Transmission electron microscopy of hydrogen effects in internally oxidized palladium-chromium alloys. *Journal of Alloys and Compounds*. 2005;406(4-6):617-620.

12. Huang XY, Mader W, Kirchheim R. Hydrogen and oxygen at metal/oxide interfaces. *Acta Metallurgica et Materialia*. 1991;39(5):893-907.